◆ Human Brain Mapping 36:1554–1566 (2015) ◆

Reduced Neural Connectivity But Increased Task-Related Activity During Working Memory in De Novo Parkinson Patients

James P. Trujillo,[1,2,3] Niels J.H.M. Gerrits,[1,4] Dick J. Veltman,[2,4] Henk W. Berendse,[4,5] Ysbrand D. van der Werf,[1,3,4] and Odile A. van den Heuvel[1,2,4]*

[1]Department of Anatomy and Neurosciences, VU University Medical Center (VUmc), Amsterdam, The Netherlands
[2]Department of Psychiatry, VUmc, Amsterdam, The Netherlands
[3]Netherlands Institute for Neuroscience, An Institute of the Royal Netherlands Academy of Arts and Sciences, Amsterdam, The Netherlands
[4]Neuroscience Campus Amsterdam (NCA), Amsterdam, The Netherlands
[5]Department of Neurology, VUmc, Amsterdam, The Netherlands

Abstract: Objective: Patients with Parkinson's disease (PD) often suffer from impairments in executive functions, such as working memory deficits. It is widely held that dopamine depletion in the striatum contributes to these impairments through decreased activity and connectivity between task-related brain networks. We investigated this hypothesis by studying task-related network activity and connectivity within a sample of de novo patients with PD, versus healthy controls, during a visuospatial working memory task. Methods: Sixteen de novo PD patients and 35 matched healthy controls performed a visuospatial *n*-back task while we measured their behavioral performance and neural activity using functional magnetic resonance imaging. We constructed regions-of-interest in the bilateral inferior parietal cortex (IPC), bilateral dorsolateral prefrontal cortex (DLPFC), and bilateral caudate nucleus to investigate group differences in task-related activity. We studied network connectivity by assessing the functional connectivity of the bilateral DLPFC and by assessing effective connectivity within the frontoparietal and the frontostriatal networks. Results: PD patients, compared with controls, showed trend-significantly decreased task accuracy, significantly increased task-related activity in the left DLPFC and a trend-significant increase in activity of the right DLPFC, left caudate nucleus, and left IPC. Furthermore, we found reduced functional connectivity of the DLPFC with other task-related

Additional Supporting Information may be found in the online version of this article.

James P. Trujillo and Niels J.H.M. Gerrits contributed equally to this work.

Ysbrand D. van der Werf and Odile A. van den Heuvel contributed equally to this work.

Author Contributions: H.W.B. and O.A.v.d.H carried out patient recruitment and inclusion. Y.D.v.d.W. and O.A.v.d.H. designed the experiment and supervised analysis, N.J.H.M.G. carried out data acquisition, and J.P.T. performed data analysis. J.P.T. and N.J.H.M.G. wrote the manuscript with technical support and conceptual advice from D.J.V., H.W.B., Y.D.v.d.W., and O.A.v.d.H. All authors contributed to the discussion of conclusions and implications of this work.

Contract grant sponsor: Neuroscience Campus Amsterdam/Institute for Clinical and Experimental Neuroscience (NCA/ICEN) and Amsterdam Brain Imaging Platform (ABIP). Financial support for this study was provided by a VIDI Grant 016.095.359 to Y.D. Van Der Werf, from the Netherlands Organization for Scientific Research (NWO).

*Correspondence to: Odile A. van den Heuvel; Department of Psychiatry, VU University Medical Center, PO Box 7057, 1007 MB, Amsterdam, The Netherlands. E-mail: oa.vandenheuvel@vumc.nl

Received for publication 17 April 2014; Revised 5 November 2014; Accepted 11 December 2014.

DOI: 10.1002/hbm.22723

Published online 17 January 2015 in Wiley Online Library (wileyonlinelibrary.com).

regions, such as the inferior and superior frontal gyri, in the PD group, and group differences in effective connectivity within the frontoparietal network. Interpretation: These findings suggest that the increase in working memory-related brain activity in PD patients is compensatory to maintain behavioral performance in the presence of network deficits. *Hum Brain Mapp 36:1554–1566, 2015.*

Key words: *n*-back; functional magnetic resonance imaging; dynamic causal modeling; generalized form of context-dependent psychophysiological interaction; compensation

INTRODUCTION

Patients with Parkinson's disease (PD) often suffer from nonmotor symptoms, including cognitive deficits, especially in the so-called executive functions [Aarsland et al. 1999; Kaasinen and Rinne 2002; Kudlicka et al. 2011; Owen 2004]. The loss of dopamine producing neurons of the substantia nigra pars compacta and ventral tegmental area [Braak and Braak, 2000; Scatton et al., 1983] results in a hypoexcitation of the frontostriatal networks that presumably underlie the executive dysfunctions, such as working memory impairment [Chudasma and Robbins, 2006; Elliot, 2003; Owen et al., 1995].

Working memory refers to the process of temporarily storing and manipulating information in the face of ongoing processing for use in goal-directed behavior [Jaeggi, et al. 2010a; Miller, et al. 1986]. An often-employed task to assess working memory capabilities is the *n*-back paradigm: a well-established task due to its reliability and the ease of manipulating processing load [Jaeggi et al., 2010b]. Neuroimaging studies have consistently shown that task performance on the *n*-back paradigm is associated with activity of the frontostriatal network (i.e., bilateral dorsolateral prefrontal cortex (DLPFC) and bilateral caudate nucleus) and frontoparietal network (i.e., bilateral inferior parietal cortex (IPC) and bilateral DLPFC [Curtis and D'Esposito, 2003; Jurado and Rosselli 2007; Landau, et al. 2009; Owen 2000; Owen, et al. 2005; Postle et al. 2000].

Adequate dopaminergic neurotransmission in the striatum also plays an important role in task performance on working memory tasks [Bäckman et al., 2011; McNab et al., 2009]. A recent study by Ekman et al [2012] reported decreased *n*-back performance in patients with PD diagnosed with mild cognitive impairment (MCI), compared with PD patients without MCI, associated with reduced levels of dopamine-transporter binding in the right caudate nucleus, as measured by single photon emission tomography (SPECT).

Cools and D'Esposito [Cools, 2011; Cools and D'Esposito, 2011] argue that optimal dopamine levels lead to a stable working memory representation by "quelling" the activity of all but the most active cells and increasing the excitability of inhibitory neurons. This results in an increased signal-to-noise ratio between neuronal populations and thus in better communication. Also functional brain imaging shows that optimal dopamine levels lead to more focused activity, whereas depletion leads to increased and more wide-spread [Monchi et al., 2007] activation which correlates positively with task errors [Mattay et al., 2002], supporting the notion of dopaminergic modulation of functional brain networks. Lower dopamine receptor stimulation in patients with PD would thus lead to an impairment in working memory updating (i.e., replacing old/irrelevant information with new/relevant information online in the working memory), and consequently a decreased working memory performance. Brittain and Brown [2014] argue in a similar fashion that dopamine depletion in PD results in decreased synchronization between neural populations in frequencies associated with information exchange, with an increase in inhibitory frequency bands. They state that dopaminergic medication normalizes this pathological synchronization and that the degree of normalization positively correlates with improvements in clinical motor scores.

These findings suggest that dopamine plays an important role in the synchronization and connectivity between brain areas. By investigating both task-related functional connectivity as well as neural activity in de novo PD patients, we can obtain a view on how PD-related neural changes relate to behavioral task performance in early PD, unbiased by dopamine replacement therapy. Methodologically, studying de novo patients is important because dopaminergic medication down-regulates dopamine receptor density in the striatum [Thobois et al., 2004], therefore, the observed effects of PD in relation to dopamine on, for example, task-related networks be may influenced by medication use.

To gain more insight into the relation between working memory capacity and task-related network connectivity in patients with PD, we measured behavioral performance and task-related neural activation in de novo PD patients during a visuospatial *n*-back task. Analyses focused on the bilateral IPC, DLPFC, and caudate nucleus, representing the most crucial areas within the frontoparietal and frontostriatal networks. In addition to the general linear model (GLM) analyses of activation, we assessed the task-related functional connectivity of the bilateral DLPFC using psychophysiological interaction [PPI O'Reilly et al., 2012] analyses and the effective connectivity between our regions-of-interest (ROIs) using dynamic causal modeling (DCM)

TABLE I. Mean and standard deviations for demographic data

	PD patients (n=16)	Controls (n=35)	P-value
Demographics			
Age	58 ± 10 (38 – 74)	56 ± 9 (38 − 70)	0.34
Sex (% male)	11 (69%)	20(57%)	0.44
Handedness (% right)	14 (88%)	31 (89%)	0.55
IQ	105 ± 19 (82 – 142)	104 ± 15 (73 – 132)	0.85
Education	5.87± 0.9 (4 – 7)	5.69± 1.1 (3 – 7)	0.54
Clinical measures			
MMSE	28.81± 0.8 (28 – 30)	29.11± 0.8 (3 – 27	0.22
MADRS	1.88± 2 (0 – 4)	0.82 ± 2 (0 – 7)	0.004
BAI	4.63 ± 3 (0 – 9)	1.6 ± 3 (0 – 10)	0.001
BDI	4.00 ± 4 (0 − 11)	2.20 ± 3 (0 − 11)	0.04
UPDRS	21.63 ± 9 (2 – 35)		
Subtype (% tremor / % akinetic)	1 (7%) / 10 (67%)		
Lateralization (% left / % right)	6 (40%) / 2 (13%)		
Hoehn & Yahr	2 (1 – 3)		
Disease duration	2.69 ± (0 – 7)		
Behavioral measures			
Total n-back accuracy	74 ± 14 (47 – 90)	82 ± 13 (58 – 100)	0.06
n-back ($n = 0$)	95.13 ± 12 (52 – 100)	98.97 ± 5 (70–100)	0.23
n-back ($n = 1$)	90.63 ± 13 (52 – 100)	93.62 ± 11 (53 – 100)	0.39
n-back ($n = 2$)	64.69 ± 24 (23 – 98)	76.52 ± 22 (28 – 100)	0.09
n-back ($n = 3$)	46.35 ± 20 (15 – 78)	59.48 ± 24 (22 – 100)	0.08

MMSE, minimal mental state examination; MADRS, Montgomery–Åsberg depression rating scale; BAI, Beck anxiety inventory; BDI, Beck depression inventory; UPDRS, unified PD rating scale.

[Friston et al., 2003]. We hypothesized that PD patients, compared with controls, would show decreased task accuracy, accompanied by decreased task-related neural activation, reduced task-related functional connectivity of the DLPFC with other task-related areas, and altered effective connectivity within the frontoparietal and frontostriatal networks.

MATERIALS AND METHODS

Participants

Twenty-five nondemented, early-stage de novo patients with PD and 40 healthy controls participated in this study. We excluded a number of participants beforehand due to an inability to perform the task (6 patients; 3 controls); these participants had difficulty understanding or carrying out the task correctly, even during training sessions. Of the participants who had performed the task in the magnetic resonance imaging (MRI) scanner, we excluded several additional participants due to poor quality of the functional MRI images (2 patients), and extreme scores on inaccuracy (more than two standard deviations from the median) in comparison with their own group (1 patient; 2 controls), rendering our total sample size 16 patients with PD (mean age: 58.3 years ± 9.5) and 35 healthy controls (mean age: 55.5 years ± 9.5) (see Table I for demographic data). Education scores represent the highest level of completed education based on the division by Verhage [1964]. Patients were diagnosed by a movement disorder specialist according to the UK PD Brain Bank criteria [Daniel and Lees, 1993] for idiopathic PD in addition to abnormal dopamine transporter single-photon emission computed tomography (DaT-SPECT) scans where available. Patients had not yet begun dopaminergic or cholinergic medication at the time of the investigation. The Unified PD Rating Scale Part III (UPDRS-III) [Fahn et al., 1987] and Hoehn and Yahr [1967] stage were administered to assess disease severity and stage, respectively. We determined disease subtype (i.e., tremor dominant/akinetic) and disease lateralisation based on these scores using the method described by Eggers et al. [2011]. All participants were screened for general cognitive status using the Mini-Mental State Examination (MMSE) [Cockrell and Folstein, 1988], depressive symptoms using the Beck Depression Inventory [BDI Beck et al., 1996] and anxiety using the Beck Anxiety Inventory (BAI) [Beck et al., 1988]. We screened for the presence of psychiatric disorders using the Structured Clinical Interview for DSM-IV Axis-I Disorders (SCID-I) (Spitzer et al., 1992]. None of the participants had a score of <24 on the MMSE, or >15 on the BDI. Handedness was assessed using the Edinburgh handedness inventory [Oldfield, 1971]. All participants provided informed consent, obtained according to the Declaration of Helsinki, and the study protocol was

reviewed and approved by the Medical Ethical Committee of the VU University Medical Center.

Working Memory Paradigm

We assessed working memory using a visuospatial version of the *n*-back task [for details, see De Vries et al., 2013]. In short, participants were visually presented with a grey diamond figure in which four large blue dots were positioned, which were randomly replaced by a yellow dot. Working memory load was increased consecutively by asking the participants to respond, using the index finger of their dominant hand, to the location of the present dot (N0), previous dot (N1), or with a delay of two (N2), or three stimuli (N3) via an MRI compatible response box. Participants were familiarized with the task in a practice session prior to the experiment.

Image Acquisition

Functional MRI data were acquired on a GE Signa HDxt 3-T MRI scanner (General Electric, Milwaukee, WI) at the VU University Medical Center using a gradient echo-planar imaging (EPI) sequence (TR = 2,100 ms; TE = 30 ms; 64 × 64 matrix; field of view = 24 cm; flip angle = 80°) with 40 ascending slices per volume (3.75 × 3.75 mm in-plane resolution; slice thickness = 2.8 mm; interslice gap = 0.2 mm), which provided whole-brain coverage. Structural scanning included a sagittal three-dimensional gradient-echo T1-weighted sequence (256 × 256 matrix; voxel size = 1 × 0.977 × 0.977 mm; 172 sections).

Data Analysis

Behavioral data

We assessed working memory performance by calculating the overall percentage of correct responses within each condition per participant. We compared the two groups using a mixed ANOVA with task-load (levels: N0/N1/N2/N3) as within-subject factor and group (levels: patients with PD/healthy controls) as between-subject factor, while using the Greenhouse-Geisser correction when the assumption of sphericity was violated.

Image processing and analysis

Preprocessing and statistical analyses were performed in SPM8 (Wellcome Department of Imaging Neuroscience, London, UK) running in Matlab (version 7.5, The MathWorks, Natick, MA, 2000). The EPI images were first slice-time corrected, then realigned to the first image and unwarped using a least squares approach and a six parameter (rigid body) spatial transformation to correct for motion. They were subsequently warped to the Montreal Neurological Institute (MNI) T1-template, using the individual T1-weighted image for estimation. Lastly, the images were smoothed with an 8 mm Gaussian kernel.

A design matrix was created to examine within-subject effects in a first level GLM. We used a block design modeling all trials within each of the four conditions with a fixed duration of 56 s. The first regressor was labeled "N0," the second "N1," the third "N2," and the fourth "N3," and the six movement parameters that were calculated during the realignment were added to the model as covariates of noninterest. The contrast of interest, the "task-effect" contrast, was defined as "N3N2N1>N0," which was used for the whole brain GLM, region of interest, generalized form of context-dependent psychophysiological interaction (gPPI) and DCM analyses to examine the effect of working memory, corrected for baseline features of the task such as visuospatial processing and motor responses.

Contrast images derived from the first level analyses were used at the second (group) level, using whole-brain voxel-wise independent *t*-tests. Brain regions were identified using the WFU-Pick Atlas [Maldjian et al., 2003]. Whole-brain statistical maps were thresholded at $P < 0.05$ corrected for family-wise errors in the main effects. Whole-brain results represent a pooled analysis of both controls and patients together (n=51) and are subsequently used as described in the proceeding sections.

Whole-brain assessment of the effect of load (N3>N2>N1>N0) showed that these results were comparable to the "task-effect" contrast, and for purposes of comprehensibility we do not discuss these results here. All subsequent analyses are based on the task-effect contrast.

Regions of interest

We defined ROIs around the peak-voxel coordinates of the main effect of working memory (i.e., N1N2N3>N0) over all subjects (N=51; see Table I in the online data supplement), using MarsBaR (http://marsbar.sourceforge.net). Spherical ROIs with a 5 mm sphere were constructed for the left and right DLPFC (BAs 9/46; right: $x = 39$, $y = 32$, $z = 31$; left: $x = -42$, $y = 26$, $z = 31$) and with a 10 mm sphere for the IPC (BA 40; right: $x = 51$, $y = -52$, $z = 40$; left: $x = -48$, $y = -49$, $z = 46$). These coordinates were used as initial starting points, after which the center of the sphere was automatically moved to the nearest local maximum using SPM8's volume of interest (VOI) utility in each participant to account for the individual variability between participants and to increase sensitivity. Each peak was manually checked to ensure it was still in the designated region.

The average parameter estimates of the whole ROI were then extracted from the task-effect contrast per participant and were subsequently compared using two-sample *t*-tests in SPSS 20 (SPSS, Chicago, IL). For these analyses we calculated a Bonferroni-adjusted alpha value using Simple Interactive Statistical Analysis (http://www.quantitativeskills.com/sisa/calculations/bonfer.htm) that took into

account the mean correlation coefficient between all ROIs to correct for multiple comparisons. The mean correlation coefficient between all six ROIs was $r = 0.48$, leading to a Bonferroni adjusted alpha value of $P = 0.02$.

Time-courses were extracted from each of the individual ROIs, using the task-effects contrast, creating VOIs for use in the connectivity analyses. These were extracted at a 0.1 threshold to ensure robust time-series.

Functional connectivity: gPPI

We assessed the task-related functional connectivity of the left and right DLPFC using a gPPI [McLaren et al., 2012; O'Reilly et al., 2012]. A PPI analysis statistically tests in a whole-brain voxel-wise manner whether areas outside the seed region are functionally connected to the seed region during the task [O'Reilly et al., 2012]. We chose gPPI, instead of the traditional PPI [Friston et al., 1997], as it allowed us to model all psychological task conditions into one first-level design, thus improving the model-fit [McLaren et al., 2012]. We used the individually determined left and right DLPFC ROIs from the GLM analysis as seed regions.

Our first-level model included the four task conditions, the four convoluted PPI terms, the time-series of the seed-region, and the six movement parameters. We again defined the contrast "N1N2N3>N0," this time using the convoluted PPI terms and leaving the psychological variable (task conditions) and movement parameters as covariates of no interest. Subjects were excluded from this analysis if no blood-oxygen-level dependent (BOLD) time-course could be extracted due to a lack of active voxels within the region of interest, or if there were no voxels that were functionally connected to the seed region. After exclusion, 15 patients and 32 controls were included in the analysis of the left DLPFC, and 14 patients and 33 controls were included for the right DLPFC.

At the second level, we compared the contrast N1N2N3>N0 between groups using an independent samples *t*-test and an uncorrected statistical threshold of $P < 0.001$ with a spatial extent threshold of $k > 5$, while masking inclusively for the main effect of task. The same analysis procedures were used for the left and right DLPFC.

Effective connectivity: DCM

To gain more insight into the connectivity within the frontoparietal (i.e., left and right DLPFC and left and right IPC) and the frontostriatal (i.e., left and right DLPFC and caudate nucleus) network, we calculated the effective connectivity using deterministic DCM [Friston et al., 2003]. In short, DCM constructs several forward-models that predict how the BOLD signal would behave if certain connections between the interacting regions are present. It tests if the signal is driven or modulated at a certain connection or specific region. After computing all models and connections, an algorithm statistically tests which model best fits the observed data.

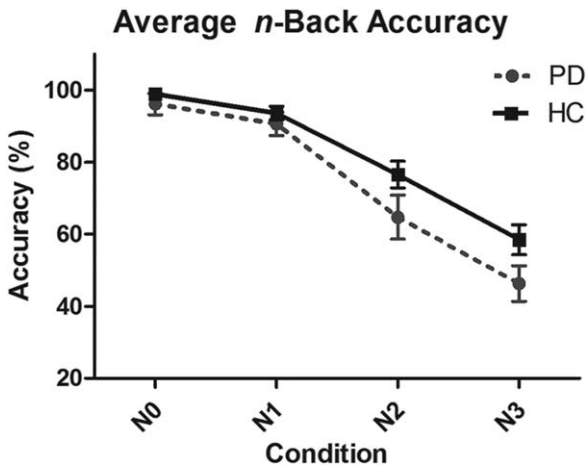

Figure 1.

Mean accuracy scores (represented on the *y*-axis), in percentages, for each group across the four conditions (displayed on the *x*-axis); The dashed line represents the PD group, and the solid line represents the healthy controls, while the error bars display the standard error of the mean. Overall a trend toward lower accuracy ($P = 0.06$) was found in the Parkinson's group. [Color figure can be viewed in the online issue, which is available at wileyonlinelibrary.com.]

For the frontostriatal network, the intrinsic connections between the left and right DLPFC were modeled in a bidirectional way, with efferent connections from each DLPFC to the ipsilateral caudate nucleus based on literature [Barbas and Pandya, 1984; Middleton and Strick, 2000]. By varying the driving and modulatory effects of working memory within the frontostriatal network, a total of seven models were created (see Supporting Information Fig. 1). For this analysis, the individually determined DLPFC VOIs, described above, were used together with time-courses extracted from masks defining the whole left and right caudate nucleus, as found in the automated anatomical labeling software package. After exclusion, the analysis included 13 patients and 34 controls.

For the frontoparietal network, intrinsic connections were again assumed to be bidirectional between left and right DLPFC, with bidirectional connections between the DLPFC and ipsilateral IPC as well as between left and right IPC. Because anatomical and functional connectivity were less clearly defined for this model-set, we generated four families of models. The families modeled top-down, bottom-up, and mixed processing, with the final family consisting of one model that utilized all possible inputs. This resulted in a total of 24 frontoparietal models (see Supporting Information Fig. 2). This analysis used the individually created VOIs for the bilateral DLPFC and IPC. After exclusion, 15 patients and 24 controls were included in this analysis.

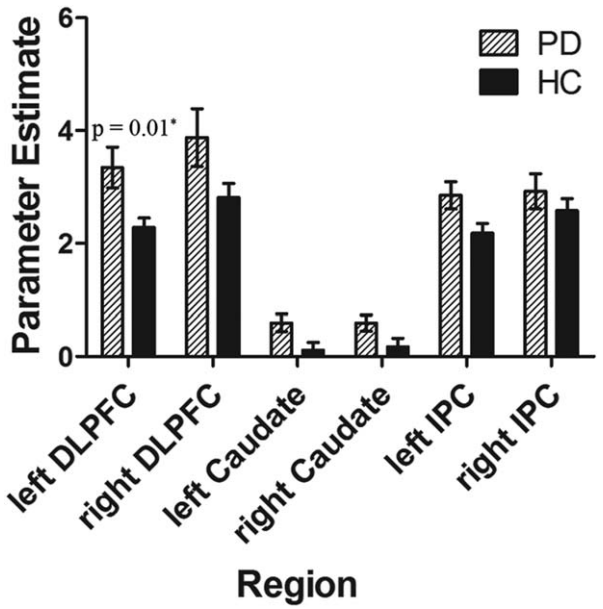

Figure 2.

Mean parameter estimates extracted from the task-effect contrast (N3N2N1>N0) per ROI per group. Shaded bars represent the PD group, while the solid bars represent the healthy controls. The *y*-axis indicates the mean parameter estimates, and the *x*-axis depicts the six ROIs. *P*-values are given for the ROIs that differed in activation between the groups. * significant after correction for multiple comparisons. Error bars represent the standard error of the mean. DLPFC, dorsolateral prefrontal cortex; IPC, inferior parietal cortex; HC, healthy controls; PD, patients with PD; ROI, region of interest. [Color figure can be viewed in the online issue, which is available at wileyonlinelibrary.com.]

We used Bayesian Model Selection (BMS) to statistically test the probability of the observed data given the model. To account for the heterogeneity of network dynamics resulting from neurodegeneration we used a random effects approach, rather than the standard fixed effects approach [Stephan et al., 2010]. Once the model-evidences have been computed for the models in each subject, the exceedance probability (Φ) can be calculated for the model-set. This is the probability that a model is more likely than any other to have generated the observed BOLD signal.

Correlation with dopamine transporter binding

For 12 out of the 16 PD patients, SPECT scans with a [^{123}I]FP-CIT tracer binding to the DaT were available with an average interval between SPECT acquisition and MRI acquisition of 55 (range: 26–123) days. We used these scans to calculate the age-corrected binding ratios (ratio of specific to nonspecific DaT binding, with the occipital lobe as a reference for nonspecific binding) in the dorsal-medial striatum (procedure and calculation described elsewhere [Vriend et al., 2013]) to perform a posthoc analysis on the relation between striatal dopamine levels and task performance (using a correlation analysis on [^{123}I]FP-CIT uptake ratios and overall task accuracy) and task-related network connectivity. We entered the [^{123}I]FP-CIT uptake ratios as covariates into a 2nd level whole-brain regression analysis of our gPPI data for both the left and right DLPFC. As this entailed an exploratory analysis, the results were considered significant at a threshold of $P < 0.001$ (uncorrected), with no spatial extent threshold.

RESULTS

The groups were matched with respect to age, gender, education, and handedness (see Table I) and did not differ on MMSE scores ($U = 336$, $P = 0.22$). PD patients, compared with healthy controls, had higher MADRS ($U = 143$, $P = 0.004$), BDI ($U = 175$, $P = 0.04$) and BAI scores ($U = 114$, $P = 0.001$), but these scores were far below accepted thresholds for mild depression or anxiety, and therefore, not clinically relevant. The mean UPDRS and median Hoehn and Yahr stage of the PD patients were 22 and two, respectively.

Behavioral Results

We found that patients with PD, compared with controls, had trend-significantly lower overall accuracy scores ($F(1,49) = 3.54$; $P = 0.06$, see Fig. 1). The accuracy scores significantly decreased with increasing task-load ($F(2.09,102.2) = 104.53$; $P < 0.001$), and this effect did not differ between patients and controls ($F(2.09,102.2) = 1.66$; $P = 0.19$).

Imaging Results

Main effect of task

The whole-brain main effect of task (contrast: N1N2N3>N0) showed significant activation of the bilateral IPC, bilateral DLPFC, bilateral ventrolateral prefrontal cortex (VLPFC), left middle frontal gyrus, left precuneus, left medial frontal gyrus, right middle temporal gyrus, bilateral posterior cingulate cortex, left superior temporal gyrus, the right cuneus, right caudate nucleus (see Supporting Information Table I). For the effect of task per group, see Supporting Information Table II; for group x task comparisons, see Supporting Information Table III.

ROI Analyses

PD patients, compared with healthy controls, showed a significant increase in task-related activation in the left DLPFC (t (21.36) = 2.65, $P = 0.01$, see Fig. 2) and a trend-significant increase in the right DLPFC (t (49) = 2.25, $P = 0.03$). The PD patients also showed a trend-significant increase in the left caudate nucleus (t (49) = 1.8, $P = 0.08$) but not in the right caudate nucleus (t (49) = 1.48,

TABLE II. Whole-brain analysis of group differences in gPPI effects for left DLPFC

			Controls > PD patients					PD patients > Controls				
					Peak coordinates (MNI)					Peak coordinates (MNI)		
	BA	Area	*T*-value	Cluster size	*X*	*Y*	*Z*	*T*-value	Cluster size	*X*	*Y*	*Z*
Positive Coupling	10	Middle frontal gyrus	5.01	36	−24	56	13					
	10		3.93	18	15	47	7					
	31	Precuneus	4.91	126	−15	−49	43					
	7		4.76		−6	−49	46					
	7		4.58		3	−37	46					
	31		3.55	16	9	−52	28					
	13	Insula	4.06	67	−48	−43	16					
	32	Anterior cingulate cortex	3.89	18	6	44	10					
	9	DLPFC	3.89	15	−36	5	34					
	8	Superior frontal gyrus	3.67	16	3	23	58					
	19	Cuneus	3.62	7	−15	−91	28					
		Putamen	3.54	6	33	−7	−11					
Negative Coupling	10	Superior frontal gyrus						5.26	173	−21	56	10
	8							3.67	13	3	23	58
	7	Precuneus						4.91	191	−15	−49	43
	7							4.58		3	−37	46
	31							3.55	17	9	−52	28
	13	Insula						4.06	141	−48	−43	16
								3.64	7	36	−13	−8
	42	Superior temporal gyrus						3.69	9	−63	−28	10
	39	Lateral occipirtal gyrus						3.79		−36	−73	13
	18	Cuneus						4.02	37	−18	−79	19
	9	Inferior frontal gyrus						3.89	5	−36	5	34
	4	Precentral gyrus						3.82	11	48	−16	37
	32	Anterior cingulate cortex						3.82	16	18	35	13

Significant at a threshold of $P = 0.001$ (uncorrected) with an extent-threshold $k > 5$.

$P = 0.15$), as well as a trend-significant increase in the left IPC (t (49) = 2.28, $P = 0.03$), but not in the right IPC (t (49) = .99, $P = 0.33$) when compared with controls.

gPPI

Compared to the PD patients, the control group showed stronger positive coupling between the left DLPFC and the bilateral middle frontal gyrus, bilateral precuneus, left insula, and the right superior frontal gyrus; no areas of stronger negative coupling were found in the controls compared with the PD patients. Patients showed no regions of stronger positive coupling compared with controls, but did show stronger negative coupling between the left DLPFC and the bilateral superior frontal gyrus, bilateral precuneus, left insula, and left inferior frontal

TABLE III. Whole-brain analysis of group differences in gPPI effects for right DLPFC

			Controls > PD patients					PD patients > Controls				
					Peak coordinates (MNI)					Peak coordinates (MNI)		
	BA	Area	*T*-value	Cluster size	*X*	*Y*	*Z*	*T*-value	Cluster size	*X*	*Y*	*Z*
Positive Coupling	47	VLPFC	3.73	5	−42	41	−2					
	6	Superior frontal gyrus	3.34	5	−6	8	67					
Negative Coupling		Cerebellum						3.89	14	0	−49	−11
	47	VLPFC						3.73	5	−42	41	−2
	47							3.62	10	33	23	−8
	6	Superior frontal gyrus						3.34	5	−6	8	67

Significant at a threshold of $P = 0.001$ (uncorrected) with an extent-threshold $k > 5$.

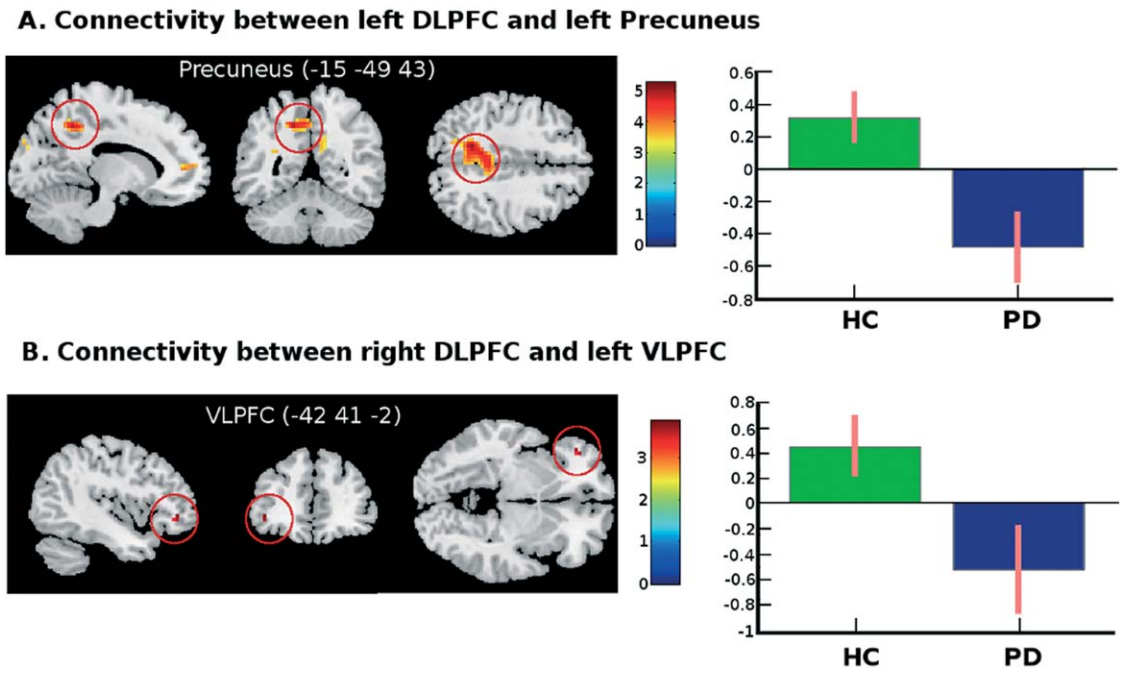

Figure 3.

Functional connectivity maps showing opposite coupling in the controls and Parkinson's patients. On the left, the cluster corresponding to a representative cluster is indicated on a standardized T1 MR image, with the name of the representative region and the peak coordinates in MNI space. The colour gradient legend represents the *Z*-scores. On the right, the bar-graph represents strength of coupling between the seed region and the representative region. Group is represented on the *x*-axis and degree of coupling on the *y*-axis. Pink lines show the standard error of the mean. **A.** Connectivity between the left DLPFC and the left precuneus. **B.** Connectivity between the right DLPFC and the left VLPFC. DLPFC, dorsolateral prefrontal cortex; HC, healthy controls; MNI, Montreal Neurological Institute; MR, magnetic resonance; PD, patients with PD; VLPFC, ventrolateral prefrontal cortex.

gyrus. Table II provides a full overview of these group comparisons and Figure 3 provides a graphic representation of how groups typically differed in coupling direction for the same regions. For the main effects of the left DLPFC within each group see Supporting Information Table IV.

The control group, compared with PD patients, showed stronger positive coupling between the right DLPFC and the left VLPFC and left superior frontal gyrus, but no stronger negative coupling. When comparing the patients with the controls, we found stronger negative coupling between the right DLPFC and the bilateral VLPFC, left superior frontal gyrus, and left cerebellum, but no stronger positive coupling. Table III provides an overview of these interaction effects. For the main effects of the right DLPFC within each group, see Supporting Information Table V.

DCM

In the frontostriatal analysis, although the exceedance probability of model two (PD: $\Phi = 0.0001$; Controls: $\Phi = 0.002$) was significantly smaller than the other six models in both groups (PD: Φ-range = 0.15–0.18; Controls: Φ-range = 0.15–0.19), no best fit model could be determined amongst the remaining six models for the healthy controls or the PD group.

Model selection of the *frontoparietal* set revealed, for the healthy controls, that model 4, that is, direct driving of the left DLPFC with modulation of the ipsilateral DLPFC/IPC connection, was the best fit ($\Phi = 0.99$). In the PD group, conversely, model 19 (driving effect of left DLPFC and left IPC; $\Phi = .64$) provided the best fit, although model 4 also had a high exceedance probability ($\Phi = 0.32$). Figure 4 shows the models with the best fit.

Dopamine Transporter Binding

Assessment of dopamine transporter binding in the dorsomedial striatum revealed a positive correlation between binding ratios and task performance, $r = .65$, $P = 0.02$ (see Fig. 5).

We also found that higher dopamine transporter binding levels in the dorsomedial striatum were associated with increased functional connectivity between the left

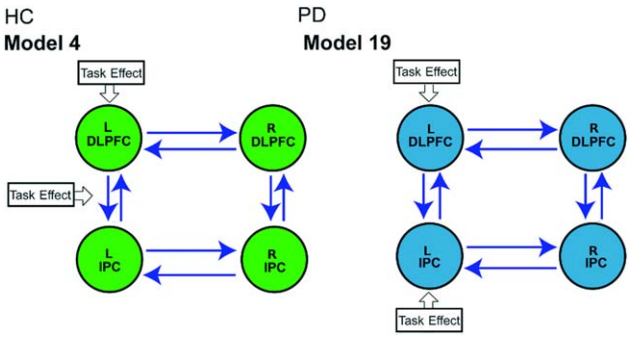

Figure 4.

Best-fit models from the frontoparietal BMS set. Circles represent the regions included in the model-space, blue arrows represent intrinsic connections, open arrows with "task effect" label pointing toward a region represent driving effects, and open arrows with the "task effect" label pointing toward intrinsic connection represent modulation of these connections. On the left: model 4, representative of the control group; on the right: model 19, representative of the patient group.

DLPFC and the bilateral middle frontal gyrus (left: $t = 6.5$; right: $t = 6.2$), the right superior parietal lobe ($t = 5.2$), and the left postcentral gyrus ($t = 4.7$).

No voxels reached the statistical threshold when investigating the relation between dopamine transporter binding ratios and functional connectivity of the right DLPFC.

DISCUSSION

This study examined the frontostriatal and frontoparietal network in unmedicated patients with PD during the performance of a visuospatial working memory task. In sum, we found that patients compared with controls displayed a mild behavioral deficit, increased task-related recruitment of the left DLPFC (related to level of dopaminergic degeneration), decreased functional connectivity of the bilateral DLPFC with other brain regions within the networks, and altered frontoparietal connectivity, with a more driving role for the IPC. These results suggest that the functional network integrity, and communication between different brain areas, is reduced in patients with PD. We hypothesize that the impaired connectivity between the task-related brain areas is caused by PD-related dopamine depletion and is compensated for by the hyperactivation of the individual task-related brain areas.

Behavioral performance in the PD patients was only marginally affected when compared with the control group. Although numerous studies reported significant impairments in working memory performance in PD patients, even in the early stages of the disease [Kehagia et al., 2010; Muslimović et al., 2005], at least one other study on working memory in unmedicated patients with PD also found no significant decrease in task-performance [Marklund et al., 2009]. Our patients had a relatively high education level (although matched with the control group) and we speculate that this might have served as a protective factor against cognitive decline [Poletti et al., 2011], either by reduced cognitive decline or increased cognitive reserves, allowing our patient group to maintain reasonably good performance.

As expected, the analyses on the combined study population, involving both patients and controls, showed a robust effect of task in the bilateral inferior parietal and prefrontal areas: areas known to be involved in working memory [Owen et al., 2005]. The PD patients, compared

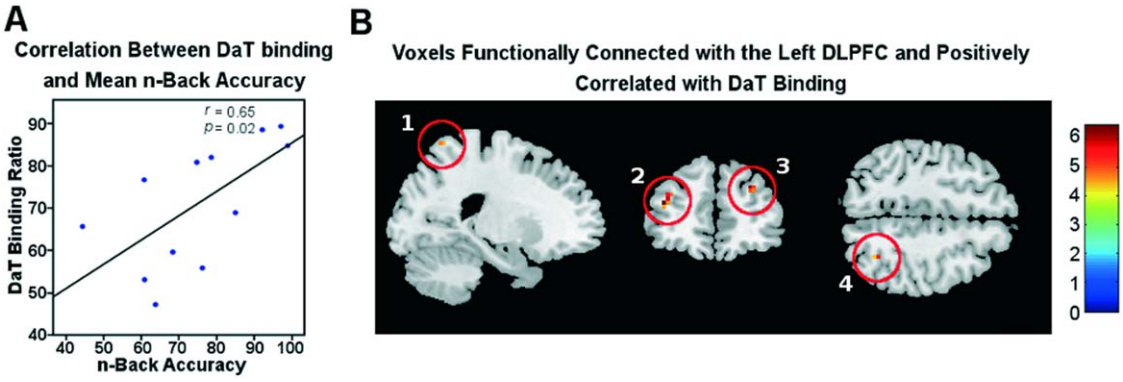

Figure 5.

Significant positive correlations between dopamine-transporter binding ratios in the dorsomedial caudate nucleus and (**A**) task performance and (**B**) functional connectivity with the left DLPFC. In A, the *y*-axis displays dopamine-transporter binding ratios, while the *x*-axis represents accuracy scores, in percentage, on the *n*-back task; B shows voxels functionally connected to the left DLPFC, as described in the gPPI analysis, which correlated positively with dopamine-transporter binding ratios. From left to right the circled regions are the left postcentral gyrus (1), the bilateral middle frontal gyrus (2–3), and the right superior parietal lobe (4).

with controls, showed significantly increased activation in the left DLPFC and a trend-wise increased activation in the right DLPFC, left caudate nucleus, and left IPC. Hyperactivation of task-related brain areas accompanied by (near) intact behavioral performance is a well-known phenomenon in both healthy aging [Grady, 2012] and disease [Clément et al., 2013; de Vries et al., 2013] and is often interpreted as a compensatory mechanism. In contrast, hypoactivation is associated with decreased task-performance (Ekman et al., 2012; Lewis et al., 2003), and we hypothesize that when the compensatory hyperactivation no longer suffices, the task-related brain areas will convert from hyper to hypoactivation and the behavioral performance will decrease accordingly.

We found that the left and right DLPFC of healthy controls, compared with PD patients, was functionally more strongly connected with prefrontal regions, the precuneus, and insula during task performance. The disease-related changes, such as the striatal dopamine depletion, likely mediate reduced functional connectivity, underscoring the important role of dopamine in orchestrating connectivity between areas during task performance. Previous studies have shown that dopamine plays an important role in enhancing the signal-to-noise ratio between assemblies of neurons [Kroener et al., 2009], and that it plays an important part in the connectivity between different brain areas [Kelly et al., 2009]. Negative coupling exists between task-related networks and the default mode network and indicates a suppression of the default mode network by the task-related network [Chen et al., 2013]. Our finding of increased negative coupling, therefore, with little to no positive coupling, within and between task-related functional networks in unmedicated PD patients provides further evidence that a decline in striatal dopamine results in highly impaired information exchange, possibly leading to inhibition within the task-related network. This pattern of connectivity reversal in PD patients compared to controls was also reported by Wu and colleagues [Wu et al., 2012]. This hypothesis is further strengthened by our positive correlation between presynaptic striatal dopamine levels and connectivity between the left DLPFC and other (prefrontal) areas.

Our group and others have found increased connectivity during rest [Olde Dubbelink et al., 2013; Silberstein et al., 2005; Stoffers et al., 2008], which seems to support the hypothesis that the inability to adequately suppress resting state networks results in the inability to switch to task-specific functional networks. A second possible explanation for the opposing direction of altered network connectivity at rest and during task performance relates to the difference in methodology of the aforementioned studies compared to this study. The mentioned resting state results were based on electroencephalogram (EEG) and magnetoencephalogram (MEG) data and concerned global connectivity in the form of oscillatory synchronization in various frequency bands. Therefore, while global connectivity is increased, connectivity within task-specific networks may be decreased. This explanation is largely in line with the theory of decreased signal-to-noise ratio as overall connectivity increases while functional efficiency decreases. As executive functioning relies on the activation of the prefrontal cortex and its ability to functionally connect with other frontal and posterior regions [Elliott, 2003], our results provide an explanatory model as to why PD patients have difficulties with working memory tasks. Although largely in agreement with our findings and hypotheses, we suggest some caution in directly comparing our study with those discussed above, as our study focused on task-related systems as measured by fMRI, while those of Olde Dubbelink [Olde Dubbelink et al., 2013], Silberstein [Silberstein et al., 2005], and Stoffers [Stoffers et al., 2008] measure the brain at rest using MEG/EEG.

The effective connectivity analyses in the healthy controls showed a best-fit with a top-down model of processing in the frontoparietal network, with the DLPFC as the main driving region and task-modulated connectivity between the DLPFC and the IPC. This result agrees with findings from another DCM study in healthy controls that also showed a modulatory effect on frontoparietal coupling in a working memory task [Ma et al., 2011]. In contrast, in patients with PD the model of best fit implies a different connectivity pattern, with both the DLPFC and IPC serving as driving regions with no task-modulated coupling. This finding fits our hypothesis that patients with PD use a different and less-connected task-related network. A recent longitudinal analysis of MEG resting state data that compared graph theoretical network properties of PD patients over time similarly showed that already in the early stages the network topology is less efficiently organized, and becomes more fragmented with increasing disease duration [Olde Dubbelink et al., 2013]. Rowe and colleagues [Rowe et al., 2002] also found that healthy participants increased effective connectivity between prefrontal and presupplementary motor areas during a motor sequence task, while the patients with PD showed no such task-specific modulation of this premotor network, suggesting a differently organized and less efficiently connected network. This altered network dynamic was also accompanied by hyperactivation of the presupplementary motor area, similar to the hyperactivation seen in conjunction with disrupted functional and effective connectivity in our own study. In that study dopaminergic medication restored the effective connections within the sample of Parkinson's patients to those of healthy controls [Rowe et al., 2010], further underscoring the role of dopamine in neural communication.

Contrary to our findings in the frontoparietal network, we found no best-fit models of effective connectivity within the frontostriatal network. Considering our hypothesized role of dopamine and the frontostriatal system, this was unexpected. This may be due to a less specific role of the caudate nucleus in performing the task compared to baseline, as recent computational theories

place the caudate nucleus in the role of action selection and updating working memory [Frank et al., 2001], disallowing a strong fit between our models and the data. The relatively small sample size used for this network, however, may also be responsible for none of the models having a better fit than the others.

We hypothesize that PD patients in our sample, still in an early disease stage, compensate for a loss in connectivity and efficiency via hyperactivation, in a way that has been previously described to mask cognitive dysfunction in patients with PD [Carbon et al., 2010; Monchi et al., 2007] as well as in multiple sclerosis patients [Hulst et al., 2012]. Eventually, cognitive impairments become behaviorally evident when hyperactivation is either no longer able, or is insufficient, to compensate for the decreased connectivity.

Previous investigations have shown that dopaminergic medication alleviates at least some cognitive dysfunctions in patients with PD [Cools, 2006] and Parkinson patients display reduced activity in the ON state when compared with the OFF state during a working memory task [Mattay et al., 2002]. We thus hypothesize that dopamine suppletion restores network connectivity and in this way cognitive performance.

Strengths and Limitations

Most previous study results are based on data from patients already on dopamine replacement therapy; as dopaminergic medication has a long-term negative effect on receptor density [Thobois et al., 2004], the de novo nature of the present PD sample was an important methodological advantage allowing a more pure investigation of the disease process. In addition to the ROI analyses, we also presented the whole brain analyses (see Supporting Information), to prevent overlooking significant findings in non-a priori hypothesized brain regions. As our sample of PD patients was relatively small, these results have to be replicated in future studies, and the causal role of dopamine in network integrity and task performance must be confirmed with an ON versus OFF medication study, or a longitudinal study on the effects of dopamine replacement therapy on task-related connectivity. As a number of patients were excluded prior to scanning due to an inability to perform the task at all, our sample may also represent a more cognitively intact subgroup, which may also partly explain the only mild behavioral deficit that we observed. Finally, although our study focused on the role of dopamine, we cannot exclude the influence of other neurotransmitters or pathological atrophy as contributing factors to our findings.

CONCLUSION

We hypothesize that the decrease in connectivity within the networks was compensated for by the hyperactivation of the individual task-related brain areas and that this compensation underlies the relatively preserved working memory task-performance.

ACKNOWLEDGMENT

The authors would like to thank Froukje de Vries, MD, for her help and useful comments during the analyses and Chris Vriend, MSc, for supplying us with the DaT-SPECT uptake ratios.

REFERENCES

Aarsland D, Larsen JP, Lim NG, Janvin C, Karlsen K, Tandberg E, Cummings JL. (1999): Range of neuropsychiatric disturbances in patients with Parkinson's disease. J Neurosurg Psychiatry 67:492–496.

Bäckman L, Nyberg L, Soveri A, Johansson J, Andersson M, Dahlin E, Neely AS, Virta J, Laine M, Rinne JO. (2011): Effects of working-memory training on striatal dopamine release. Science 333:718–718.

Barbas H, Pandya DN. (1984): Topography of commissural fibers of the prefrontal cortex in the rhesus monkey. Exp Brain Res 55:187–191.

Beck AT, Epstein N, Brown G, Steer RA. (1988): An inventory for measuring clinical anxiety: psychometric properties. J Consult Clin Psychol 56:893–897.

Beck AT, Steer RA, Brown GK. 1996. Manual for the Beck Depression Inventory II. San Antonio, TX: Psychological Corporation.

Braak H, Braak E. (2000): Pathoanatomy of Parkinson's disease. J Neurol 247:II3–II10.

Brittain J-S, Brown P. (2014): Oscillations and the basal ganglia: Motor control and beyond. Neuroimage 85:637–647.

Carbon M, Reetz K, Ghilardi M, Dhawan V, Eidelberg G. (2010): Early Parkinson's disease: Longitudinal changes in brain activity during sequence learning. Neurobiol Dis 37:455–460.

Chen AC, Oathes DJ, Chang C, Bradley T, Zhou ZW, Williams LM, Glover GH, Deisseroth K, Etkin A. (2013): Causal interactions between fronto-parietal central executive and default-mode networks in humans. Proc Natl Acad Sci USA 110: 19944–19949.

Chudasama, Y, Robbins, TW (2006): Functions of frontostriatal systems in cognition: comparative neuropsychopharmacological studies in rats, monkeys and humans. Biological psychology 73:19–38.

Clément F, Gauthier S, Belleville S. (2013): Executive functions in mild cognitive impairment: Emergence and breakdown of neural plasticity. Cortex 49:1268–1279.

Cockrell JR, Folstein MF. (1988): Mini-mental state examination (MMSE). Psychopharmacol Bull 24:689–692.

Cools R. (2006): Dopaminergic modulation of cognitive function-implications for L-DOPA treatment in Parkinson's disease. Neurosci Biobehav Rev 30:1–23.

Cools R. (2011): Dopaminergic control of the striatum for high-level cognition. Curr Opin Neurobiol 21:402–407.

Cools R, D'Esposito M. (2011): Inverted-U-shaped dopamine actions on human working memory and cognitive control. Biol Psychiatry 69:e113–e125.

Curtis, CE, D'Esposito, M. (2003): Persistent activity in the prefrontal cortex during working memory. Trends in cognitive sciences 7:415–423.

Daniel SE, Lees AJ. (1993): Parkinson's disease society brain bank, London: overview and research. J Neural Transm Suppl 39: 165–172.

de Vries FE, de Wit SJ, Cath DC, van der Werf YD, van der Borden V, van Rossum TB, van Balkom AJLM, van der Wee NJA, Veltman DJ, van den Heuvel OA: Compensatory frontoparietal activity during working memory: An endophenotype of obsessive-compulsive disorder. Biol Psychiatry 76: 878–887.

Eggers C, Kahraman D, Fink GR, Schmidt M, Timmerman L. (2011): Akinetic-rigid and tremor-dominant Parkinson's disease patients show different patterns of FP-CIT single photon emission computed tomography. Mov Disord 26:416–423.

Ekman U, Eriksson J, Forsgren L, Mo SJ, Riklund K, Nyberg L. (2012): Functional brain activity and presynaptic dopamine uptake in patients with Parkinson's disease and mild cognitive impairment: A cross-sectional study. Lancet Neurol 11:679–687.

Elliott R. (2003): Executive functions and their disorders imaging in clinical neuroscience. Br Med Bull 65:49–59.

Fahn S, Elton RL, Committee MotUD. 1987. Unified Parkinson's disease rating scale. In: Fahn S, Marsden CD, Calne D, Goldstein M, editors. Recent Developments in Parkinson's Disease. Florham Park, NJ: Macmillan Healthcare Information. pp 153/164.

Frank MJ, Loughry B, O'Reilly RC. (2001): Interactions between frontal cortex and basal ganglia in working memory: A computational model. Cogn Affect Behav Neurosci 1:137–160.

Friston K, Harrison L, Penny W. (2003): Dynamic causal modelling. NeuroImage 19:1273–1302.

Friston KJ, Buechel C, Fink GR, Morris J, Rolls E, Dolan RJ. (1997): Psychophysiological and modulatory interactions in neuroimaging. Neuroimage 6:218–229.

Grady C. (2012): The cognitive neuroscience of ageing. Nat Rev Neurosci 13:491–505.

Hoehn MM, Yahr MD. (1967): Parkinsonism: Onset, progression and mortality. Neurology 17:427–442.

Hulst H, Schoonheim M, Roosendaal S, Popescu V, Schweren L, van der Werf Y, Visser L, Polman C, Barkhof F, Geurts J. (2012): Functional adaptive changes within the hippocampal memory system of patients with multiple sclerosis. Hum Brain Mapp 33:2268–2280.

Jaeggi S, Buschkuehl M, Perrig W, Meier B. (2010a): The concurrent validity of the N-back task as a working memory treasure. Memory 18:394–412.

Jaeggi SM, Buschkuehl M, Perrig WJ, Meier B. (2010b): The concurrent validity of the N-back task as a working memory measure. Memory 18:394–412.

Jurado MB, Rosselli M. (2007): The elusive nature of executive functions: a review of our current understanding. Neuropsychology review 17:213–233.

Kaasinen V, Rinne JO. (2002): Functional imaging studies of dopamine system and cognition in normal aging and Parkinson's disease. Neurosci Behav Rev 26:785–793.

Kehagia AA, Barker RA, Robbins TW. (2010): Neuropsychological and clinical heterogeneity of cognitive impairment and dementia in patients with Parkinson's disease. Lancet Neurol 9: 1200–1213.

Kelly C, de Zubicaray G, Di Martino A, Copland DA, Reiss PT, Klein DF, Castellanos FX, Milham MP, McMahon K. (2009): L-dopa modulates functional connectivity in striatal cognitive and motor networks: A double-blind placebo-controlled study. J Neurosci 29:7364–7378.

Kroener S, Chandler LJ, Phillips PEM, Seamans JK. (2009): Dopamine modulates persistent synaptic activity and enhances the signal-to-noise ratio in the prefrontal cortex. PLoS One 4: e6507.

Kudlicka A, Clare L, Hindle JV. (2011): Executive functions in Parkinson's disease: Systematic review and meta-analysis. Mov Disord 26:2305–2315.

Landau SM, Lal R, O'Neil JP, Baker S, Jagust WJ (2009): Striatal dopamine and working memory. Cerebral Cortex 19: 445–454.

Lewis SJG, Dove A, Robbins TW, Barker RA, Owen AM. (2003): Cognitive impairments in early Parkinson's disease are accompanied by reductions in activity in frontostriatal neural circuitry. J Neurosci 23:6351–6356.

Ma L, Steinberg JL, Hasan KM, Narayana PA, Kramer LA, Moeller FG. (2011): Working memory load modulation of parieto-frontal connections: Evidence from dynamic causal modeling. Hum Brain Mapp 33:1850–1867.

Maldjian JA, Laurienti PJ, Kraft RA, Burdette JH. (2003): An automated method for neuroanatomic and cytoarchitectonic atlas-based interrogation of fMRI data sets. Neuroimage 19:1233–1239.

Marklund P, Larsson A, Elgh E, Linder J, Riklund KÃhm, Forsgren L, Nyberg L. (2009): Temporal dynamics of basal ganglia under-recruitment in Parkinson's disease: Transient caudate abnormalities during updating of working memory. Brain 132:336–346.

Mattay VS, Tessitore A, Callicott JH, Bertolino A, Goldberg TE, Chase TN, Hyde TM, Weinberger DR. (2002): Dopaminergic modulation of cortical function in patients with Parkinson's disease. Ann Neurol 51:156–164.

McLaren DG, Ries ML, Xu G, Johnson SC. (2012): A generalized form of context-dependent psychophysiological interactions (gPPI): A comparison to standard approaches. Neuroimage 61: 1277–1286.

McNab F, Varrone A, Farde L, Jucaite A, Bystritsky P, Forssberg H, Klingberg T. (2009): Changes in cortical dopamine D1 receptor binding associated with cognitive training. Science 323:800–802.

Middleton FA, Strick PL. (2000): Basal ganglia and cerebellar loops: Motor and cognitive circuits. Brain Res Rev 31:236–250.

Miller GA, Galanter E, Pribram KH. 1986. Plans and the Structure of Behavior. New York: Adams Bannister Cox.

Monchi O, Petrides M, Mejia-Constain B, Strafella AP. (2007): Cortical activity in Parkinson's disease during executive processing depends on striatal involvement. Brain 130:233–244.

Muslimović D, Post B, Speelman JD, Schmand B. (2005): Cognitive profile of patients with newly diagnosed Parkinson disease. Neurology 65:1239–1245.

O'Reilly JX, Woolrich MW, Behrens TEJ, Smith SM, Johansen-Berg H. (2012): Tools of the trade: Psychophysiological interactions and functional connectivity. SCAN 7:604–609.

Olde Dubbelink KTE, Stoffers D, Deijen JB, Twisk JWR, Stam CJ, Berendse HW. (2013): Cognitive decline in Parkinson's disease is associated with slowing of resting-state brain activity: A longitudinal study. Neurobiol Aging 34:408–418.

Oldfield RC. (1971): The assessment and analysis of handedness: The Edinburgh inventory. Neuropsychologia 9:97–113.

Owen AM. (2004): Cognitive dysfunction in Parkinson's disease: The role of frontostriatal circuitry. Neuroscientist 10:525–537.

Owen AM, Sahakian BJ, Hodges JR, Summers BA, Polkey CE, Robbins TW (1995): Dopamine-dependent frontostriatal planning deficits in early Parkinson's disease. Neuropsychology 9: 126–140.

Owen AM, McMillan KM, Laird AR, Bullmore E. (2005): N-back working memory paradigm: A meta-analysis of normative functional neuroimaging studies. Hum Brain Mapp 25:46–59.

Poletti M, Emre M, Bonuccelli U. (2011): Mild cognitive impairment and cognitive reserve in Parkinson's disease. Parkinsonism Relat Disord 17:579–586.

Postle BR, Stern CE, Rosen BR, Corkin S (2000): An fMRI investigation of cortical contributions to spatial and nonspatial visual working memory. NeuroImage 11:409–423.

Rowe JB, Stephan KE, Friston KJ, Frackowiak R, Lees AJ, Passingham R. (2002): Attention to action in Parkinson's disease: Impaired effective connectivity among frontal cortical regions. Brain 152:276–289.

Rowe JB, Hughes LE, Barker RA, Owen AM. (2010): Dynamic causal modelling of effective connectivity from fMRI: Are results reproducible and sensitive to Parkinson's disease and its treatment? Neuroimage 52:1015–1026.

Scatton B, Javoy-Agid F, Rouquier L, Dubois B, Agid Y. (1983): Reduction of cortical dopamine, noradrenaline, serotonin and their metabolites in Parkinson's disease. Brain Res 275:321–328.

Silberstein P, Pogosyan A, Kühn AA, Hotton G, Tisch S, Kupsch A, Dowsey-Limousin P, Hariz MI, Brown P. (2005): Cortico-cortical coupling in Parkinson's disease and its modulation by therapy. Brain 128:1277–1291.

Spitzer RL, Williams JB, Gibbon M, First MB. (1992): The structured clinical interview for DSM-III-R (SCID). I: History, rationale, and description. Arch Gen Psychiatry 49: 624–629.

Stephan K, Penny W, Moran R, den Ouden H, Daunizeau J, Friston K. (2010): Ten simple rules for dynamic causal modeling. NeuroImage 49:3099–3109.

Stoffers D, Bosboom JLW, Deijen JB, Wolters EC, Stam CJ, Berendse HW. (2008): Increased cortico-cortical functional connectivity in early-stage Parkinson's disease: An MEG study. NeuroImage 41:212–222.

Thobois S, Vingerhoets F, Fraix V, Xie-Brustolin J, Mollion H, Costes N, Mertens P, Benabid A-L, Pollak P, Broussolle E. (2004): Role of dopaminergic treatment in dopamine receptor down-regulation in advanced Parkinson disease: A positron emission tomographic study. Arch Neurol 61:1705–1709.

Verhage F. 1964. Intelligentie en leeftijd: Onderzoek bij Nederlanders van twaalf tot zevenenzeventig jaar [Intelligence and Age: Research in Dutch Persons Age Twelve to Seventy-Seven Years]. Assen: Van Gorcum.

Vriend C, Raijmakers P, Veltman DJ, van Dijk KD, van der Werf YD, Foncke EM, Smit JH, Berendse HW, van den Heuvel OA: Depressive symptoms in Parkinson's disease are related to reduced [123I]FP-CIT binding in the caudate nucleus. J Neurol Neurosurg Psychiatry 85:159–164.

Wu T, Wang J, Wang C, Hallett M, Zang Y, Wu X, Chan P. (2012): Basal ganglia circuit changes in Parkinson's disease patients. Neurosci Lett 524:55–59.